Research Repository UCD

Title	An Analysis on PV Forecast Allocation for Distribution System Planning
Authors(s)	Rigoni, Valentin, Melhorn, Alexander C., Keane, Andrew, Taylor, Jason
Publication date	2019-09-02
Publication information	Rigoni, Valentin, Alexander C. Melhorn, Andrew Keane, and Jason Taylor. "An Analysis on PV Forecast Allocation for Distribution System Planning." IEEE, September 2, 2019. https://doi.org/10.1109/ISGTEurope.2019.8905670.
Conference details	The 2019 IEEE PES Innovative Smart Grid Technologies Europe (ISGT-Europe), Bucharest, Romania, 29 September - 2 October 2019
Publisher	IEEE
Item record/more information	http://hdl.handle.net/10197/26113
Publisher's statement	© 2019 IEEE. Personal use of this material is permitted. Permission from IEEE must be obtained for all other uses, in any current or future media, including reprinting/republishing this material for advertising or promotional purposes, creating new collective works, for resale or redistribution to servers or lists, or reuse of any copyrighted component of this work in other works.
Publisher's version (DOI)	10.1109/ISGTEurope.2019.8905670

Downloaded 2026-05-02 00:24:56

The UCD community has made this article openly available. Please share how this access benefits you. Your story matters! (@ucd_oa)

© Some rights reserved. For more information

An Analysis on PV Forecast Allocation for Distribution System Planning

Valentin Rigoni
Andrew Keane
University College Dublin
Dublin, Ireland
valentin.rigoni@ucdconnect.ie; andrew.keane@ucd.ie

Alexander C. Melhorn
Jason Taylor
Electric Power Research Institute
Knoxville, TN, USA
amelhorn@epri.com; jtaylor@epri.com

***Abstract*—As the adoption of residential photovoltaic (PV) continues to increase, its influence on distribution feeder voltage and currents also increases. Effective allocation or modelling on the appearance of PV across the system as a function of an adoption forecast is an important consideration for future distribution planning. The spatial information required for the forecast/allocation process is expected to be available to utilities at a cost proportional to its level of detail. Naturally, there is a need to understand the potential trade-offs between different modelling approaches and options. This paper explores three allocation models that differ on the complexity of their allocation mechanism. Both the error due to ignoring customers' PV adoption mechanisms and due to the PV forecast uncertainty are explored and compared.**

***Index Terms*-- Distributed generation, Forecasting, Power distribution, Power system planning, Renewable energy sources**

I. INTRODUCTION

The technical impacts that distributed energy resources (DER) can have on distribution networks have been widely addressed by existing literature [1]–[4]. Therefore, utilities are looking to incorporate DER into their network planning techniques. One of the main challenges is the evaluation of the branch power flows that can result from residential photovoltaics (PVs) at the distribution level; which can improve the identification of potential assets overloading.

The estimation of future branch power flows has been a matter of study for distribution planners before the advent of DER. For instance, the concept of growth behaviour as a function of spatial resolution is used to assess the increment, over time, of the demand in distribution networks [5]. When incorporating PVs, utilities are expected to follow similar methodologies. The reverse branch power flows related to a PV generation forecast in a distribution feeder can be estimated by allocating the forecast at the customer level based on the available spatial information; allowing for planning actions if the network integrity is expected to be jeopardized. Given that the cost of providing such spatial information is expected to be proportional to its level of detail, utilities must consider the latter based on their use-case requirements [6]. For instance, the required level of detail pertaining to customer characterization is expected to be lower at the substation level compared to that needed to assess system performance for assets serving a few customers close to the ends of the system. In the first case, all the allocations would be aggregated together, making the characteristics of each individual customer irrelevant. On the other hand, estimating the power flows at low levels of granularity may prove unjustifiable given inherent uncertainties and relatively higher labor costs associated with proactive measures at these levels of the system.

Three different PV allocation models are examined, namely: uniform, random and spatial allocation. They differ on the power allocated per customer and on the type of PV adoption mechanism (i.e., the way customers adopt PV). The uniform allocation is considered as a base case and compared with the other two to analyse the variation on the branch power flows that can take place under more realistic allocations. The PV forecast error is also considered, and the resultant error propagation is compared with the previous variations (due to the utilized allocation models). This study can help utilities to identify which feeder branches are more sensitive to the PV forecast quality or to the customer characterization detail; providing information concerning under which conditions the need for more detailed information, on customer characteristics and/or expected PV adoption mechanism, is justifiable.

II. METHODOLOGY

An allocation is understood here as a predetermined way of distributing a PV forecast given at the head of the feeder among the feeder's customers. This process depends on the information that is available to utilities. For instance, allocations can be derived from customer/location-based information, service transformer data, or simply from network topology with no extra knowledge; similar to demand allocation [6]. Nonetheless, the quality of prior information will have an impact on the accuracy of the allocation and therefore, on the subsequent planning decisions [1]. Three different allocation models are outlined in this section, with incremental levels of complexity. For all models, it is assumed that the total PV active power generation forecast is available at the head of the feeder.

A. Uniform Allocation Model

In the uniform allocation model, all customers adopt an equal share of the total PV forecast. Consequently, the PV power allocation at each customer, p_c, is the same and is obtained by dividing the total power forecast at the head of the feeder, P_F, by the total number of customers, N:

This work was carried out at the Electric Power Research Institute and has been supported by its members. V. Rigoni and A. Keane are supported by Science Foundation Ireland under the SFI Strategic Partnership Programme Grant Number SFI/15/SPP/E3125.
978-1-5386-8218-0/19/$31.00 ©2019 IEEE

Accepted Paper

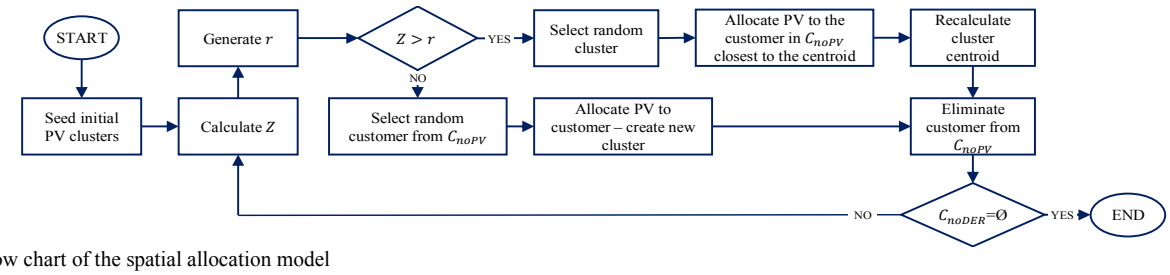

Fig. 1. Flow chart of the spatial allocation model

$$p_c = P_F / N \quad (1)$$

Uniform allocation results in no diversity among customers. While not expected to hold true in reality, such allocation is expected to be relatively accurate when aggregating high numbers of customers [2]. Therefore, uniform allocation can be considered as a practical assumption when there is a lack of customer characterization and/or spatial information. Here, the uniform allocation is used as a benchmark to assess the power flow fluctuations that can be expected when considering the more realistic PV adoption mechanisms in the other two allocation models. The objective is to help utilities to determine the need for detailed spatial customer characterization.

B. Random Allocation Model

Uniform power allocations will not hold true in most cases as PV power injections vary according to the geographical location and installed capacity. Therefore, the random allocation model incorporates diversity on the value of the allocated power injection to explore how it can affect the trend of the branch power flows. Given a feeder with n_{PV} PVs, the process for a single allocation simulation is as follows:

1. Randomly select n_{PV} customers from the feeder. The selection process has no preference for any given customer.
2. Each one of the selected customers is allocated with a discrete PV power injection. The allocated power is randomly selected from a pool of typical PV system sizes from historical data. Once allocated, the sum of the power injections from all customers with PV is equal to the forecast at the head of the feeder.

As the customers with PV and their allocated power injections are randomly selected, every allocation simulation will result in different branch power flows. To capture this, a Monte Carlo (MC) analysis is applied [7]. The process from the two previous steps is repeated for each MC iteration and all the resulting flows are stored for a latter assessment.

C. Spatial Allocation Model

In the previous allocations, there is no customer differentiation based on geographical location as all customers have the same probability of being allocated with PV. However, the inclusion of new PV systems may depend on how PVs are adopted over time; as observed in [8]. In that study, the probability of a customer to adopt PV is found to be greater under the presence of existing PV in the surrounding area.

The spatial allocation model strives to capture PV adoption as a function of the spatial characteristics and is summarized in Fig. 1. It mimics the trends observed in [5],[8]. The algorithm starts with a random seed of PV systems defined as initial adoption clusters. Every cluster is characterized by a centroid, i.e. the mean geographical coordinates of all its customers. Then, for every new PV, a probability Z of creating a new cluster is calculated as a function of the current amount of PV in the system. Next, a random number r is generated from a uniform probability distribution, with $0 \leq r \leq 1$, and is compared with Z. If $Z > r$, a random existing cluster is selected and the customer (from the set of customers with no PV, C_{noPV}) with the smallest distance to the cluster's centroid is identified, allocated with a PV power injection and added to the cluster. If $Z \leq r$, a PV power injection is allocated to a random customer, from C_{noPV}, which becomes a new cluster. In each case, the selected customer is eliminated from C_{noPV}; stopping allocations when the sum of allocated powers equals the total PV forecast. Power allocations are randomly selected based on typical PV capacities; same as the random allocation model. The model is implemented with a MC analysis where each execution of the flow chart in Fig. 1 results in different values of the allocated PV for each customer.

III. Case Study

The three allocation models are implemented on the Electric Power Research Institute (EPRI) test circuit 5 [9], depicted in Fig. 1. The radial distribution feeder supplies 1,379 customers distributed among 585 service transformers (i.e. blue circles). The head of the feeder (i.e. red triangle) is connected to the primary substation's secondary busbar. While a typical US distribution feeder is used, the methodology is sufficiently general, and deductions from the obtained results can be considered independently of the circuit model. The study case focuses on residential PV, but the proposed method can be extended to any DER. It is assumed that the PV active power forecast is available at the feeder head and, regardless of the allocation model, the sum of all allocated injections equals the forecasted value. Reactive power, system demand and losses are neglected. For both random and spatial allocations, the allocated power injections are randomly selected from the typical PV sizes in [10], where discrete values of 1.0, 1.5, 2.0, 2.5, 3.0, 3.5 and 4.0 kW; have a probability of 1, 8, 13, 14, 12, 37 and 15% of being adopted respectively.

The amount of PV in the system will be characterized by the PV penetration level, $PV_{\%}$. Interpreted as the percentage of feeder customers that have PV, $PV_{\%}$ provides a quantification of the presence of PV in the system, independent of the actual value of the allocated powers. Therefore, it is suitable for a sensitivity analysis on the trend of the obtained results.

IV. Results

A. Uniform Allocation

The uniform allocation is implemented at 25, 50, 75 and 100% PV penetration (i.e. PV forecasts of 1042.5, 2067, 3093.5 and 4141 kW respectively). Both the reverse and normalized

Accepted Paper

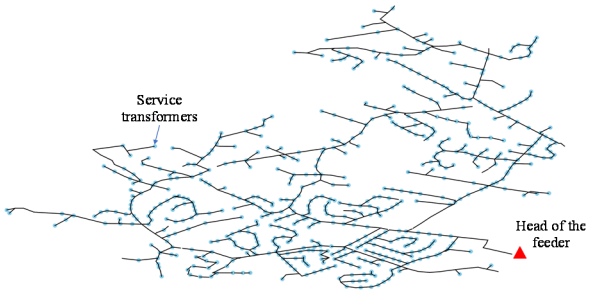

Fig. 2. EPRI circuit 5 – 585 service transformers and 1,379 customers

reverse active power flows against the number of downstream customers, n_{cust}, for the listed $PV_{\%}$ across all the branches of the feeder are plotted in Fig. 3. The power flows observed in Fig. 3 (a) monotonically increment with n_{cust} and converge to the total forecast when $n_{cust} \rightarrow N$. Regression analysis [11] is used to fit these flows with the linear model:

$$\hat{P}_{flow} = b_1 \times n_{cust} + b_2 \quad (2)$$

The values for b_1 and b_2 and R^2 correlation [11] are listed in Table I. A perfect correlation (R^2=1) is observed between the variables in the two axes for all $PV_{\%}$ values for the uniform allocation as both p_c from (1) and b_1 represent the increment on a branch power flow when aggregating an extra customer. Fig. 3 (b) shows the normalized active power flow versus n_{cust}, which corresponds the mean of the power allocated across the customers downstream a branch. These normalized flows are constant and equivalent to the slopes in Table I. The points sparsity in Fig. 3 is due to n_{cust} not belonging to a continuous space (i.e., branches feeding all possible customers counts does not occur in the feeder). As a general outcome, given that all customers take an equal share of the PV forecast, there is no variability on the obtained flows at any point of the system.

B. Random Allocation

The random allocation is implemented with 2,500 MC iterations. Both the reverse and normalized reverse active power flows against n_{cust} for a 50% PV penetration, across all branches, are plotted in Fig. 4. Each dot represents the total reverse or normalized reverse active power flow at a branch with n_{cust} downstream customers over all the MC iterations. The linear model proposed in (2), dashed line in Fig. 4 (a), is used to fit the trend of the obtained flows. Table I shows the values for R^2, and b_1 and b_2 coefficients at a 25, 50, 75 and 100% PV penetration. The obtained parameters are almost equal to those from the uniform allocation. This equivalence is important. It expresses that the obtained linear model represents the power flows from a uniform allocation model. The model (2) will be used for the later comparison between allocations.

The obtained reverse power flows and normalized reverse power flows are shown in Fig. 4 (a) and Fig. 4 (b) respectively. In both cases, there is variability among branches with the same n_{cust}. The variability is due to the model's stochastic nature, where each customer at each MC iteration can be allocated with different PV capacities or no PV. Fig. 4 (b) shows that variability increases when approaching the feeder's ending branches, this is because the characteristics of each individual allocation are more noticeable when the number of aggregated customers is low. For instance, for branches with a single customer, the allocated power can go from zero to any of the considered PV capacities. As more customers are aggregated,

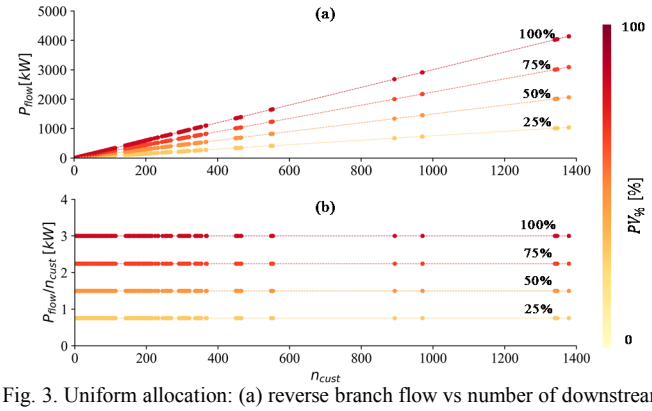

Fig. 3. Uniform allocation: (a) reverse branch flow vs number of downstream customers and (b) normalized branch flow vs number of downstream customers at 25%, 50%, 75% and 100% penetration levels.

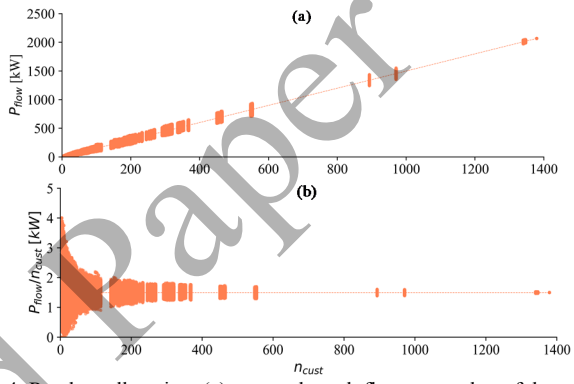

Fig. 4. Random allocation: (a) reverse branch flow vs number of downstream customers and (b) normalized reverse branch flow vs number of downstream customers at 50% penetration level (i.e., $P_F = 2067kW$).

TABLE I
MODEL (2) RESULTS FOR THE BRANCH FLOWS IN FIG. 4

$PV_{\%}$ [%]	Uniform Allocation			Random Allocation			Spatial Allocation		
	b_1	b_2	R^2	b_1	b_2	R^2	b_1	b_2	R^2
25	0.76	0.00	1	0.76	0.01	0.997	0.75	0.02	0.984
50	1.50	0.00	1	1.50	0.00	0.998	1.50	0.03	0.994
75	2.24	0.00	1	2.24	0.01	0.998	2.25	0.02	0.997
100	3.00	0.00	1	3.00	0.00	0.998	3.00	0.00	0.999

the normalized power flows converge to the allocated power p_c in (1) from the uniform allocation (1.50kW, for a 50% penetration). In addition, the trend of the normalized flow variation around the offset presents a knee-point for n_{cust} between 0 and 100; which limits the branches from which the aggregated allocations start significantly diverging from the assumption of a uniform PV adoption.

C. Spatial allocation

The spatial allocation model is implemented with 2,500 MC iterations, with each iteration being initialized with a random seed of 10 PV units. Z is modelled with the sigmoid function:

$$Z = 1 \Big/ \left(1 + e^{-[PV_{\%} \times 12 - 6]}\right) \quad (3)$$

This function, plotted in Fig. 5, simulates the transition from an initial stage, with new PVs being more likely adopted in areas with existing PV, to a final stage with PVs being equally adopted at any location.

Reverse and normalized reverse active power flows against n_{cust} for a 50% PV penetration, across all branches, are plotted in Fig. 6. After fitting (2) to the calculated branch power flows,

Accepted Paper

an equivalence with the uniform allocation model is again listed in Table I. From Fig. 6, it is clear that branch power flows variations are greater than those obtained from the random allocation in Fig. 4. The increase in variability is expected because the spatial allocation model does not only randomize the allocated powers' value but incorporates a location dependent PV adoption mechanism, which can lead to the presence of large adoption clusters at specific feeder sections. The increase in variability contributes to the normalized branch flows in Fig. 6 (b) converging to the offset from the uniform allocation at a lower rate compared to the random allocation. For instance, the average allocated power can fluctuate between approximately 0.3 and 3 kW at branches with up to 300 downstream aggregated customers (against the ~1.1-1.9 kW observed with the random allocation).

D. Comparing Allocations

The difference in the branch reverse power flows for the random and spatial allocation models with respect to the uniform allocation model is defined as:

$$\Delta P_{flow}[kW] = P_{flow} - \hat{P}_{flow} \tag{4}$$

where P_{flow} is the calculated reverse power flows and $\hat{P}_{flow}$ the predictions from (2). Histograms for ΔP_{flow} for the random allocation model at $n_{cust} = 200$ are shown in Fig. 7. Results follow a normal distribution with $\mu \approx 0$, i.e. the uniform allocation is at the centre of the distribution. When comparing the histograms at $PV_{\%} = 5$ and 100% to those at $PV_{\%} = 25$ and 75%, it can be noticed that the distribution of ΔP_{flow} is more skewed when approaching the penetration upper and lower limits (i.e., 0% and 100%). ΔP_{flow} may be expected to increase proportionally with $PV_{\%}$ (there is more power to be allocated). However, at high penetration levels, ΔP_{flow} shows to decrease. The decrease occurs because there is low sparsity of the allocations when most of customers have PV; which results on P_{flow} approaching the flows from a uniform allocation. The same observations can be made for the spatial allocation model.

If ΔP_{flow}, is interpreted as the error that may take place under the assumption of a uniform allocation, it is of interest to quantify it in terms of percentage difference:

$$\Delta P_{flow}[\%] = \frac{P_{flow} - \hat{P}_{flow}}{\hat{P}_{flow}} \times 100 \tag{5}$$

Fig. 8 depicts the 90th and 10th percentile of the percent differences for the random allocation (from the distribution of the results from all the Monte Carlo simulations) against the number of aggregated customers at various PV penetrations. From an allocation accuracy perspective, it can be said that the need of low granularity spatial characterization becomes more evident when approaching the ending branches of the feeder. Additionally, incrementing the PV penetration leads to reduction of $\Delta P_{flow}[\%]$; as a result of lower allocation sparsity. That is, the required level of spatial characterization detail decreases with customer aggregation and with the amount of PV, a crucial observation for utilities when deciding where to focus their resources. For instance, if the interest is on the ending branches of a feeder, i.e. high $\Delta P_{flow}[\%]$, detailed spatial characterization is justifiable. However, the latter is expected to be uncommon given that most utilities typically

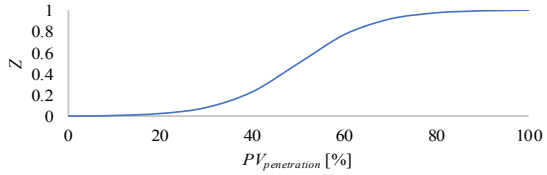

Fig. 5. Sigmoid function for the spatial allocation diffusion mechanism

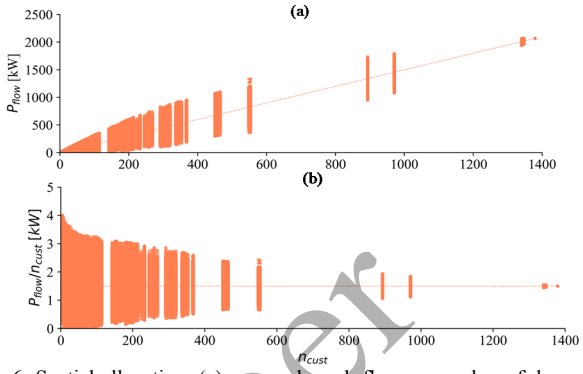

Fig. 6. Spatial allocation: (a) reverse branch flow vs number of downstream customers and (b) normalized reverse branch flow vs number of downstream customers at 50% penetration level (i.e., $P_F = 2067kW$).

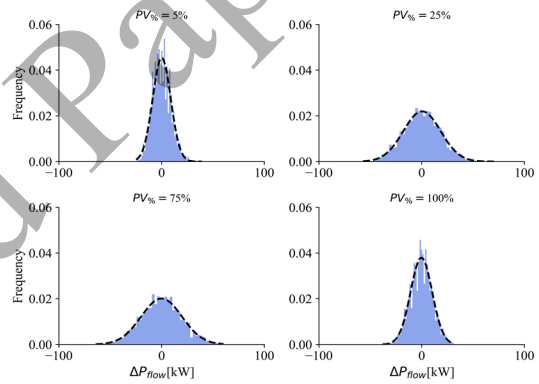

Fig. 7. Histograms and normal distribution fit for ΔP_{flow} (5) for the random allocation model and $n_{cust} = 200$.

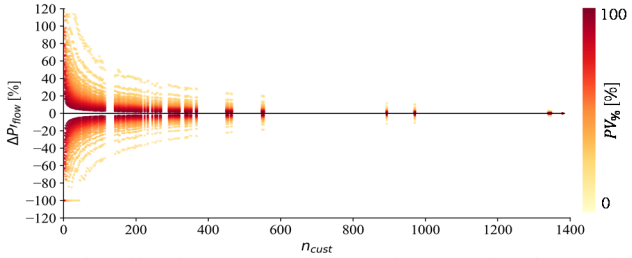

Fig. 8. Random allocation: ΔP_{flow} against n_{cust} for penetrations that vary from 5% to 100% with a 5% step for both 90th and 10th percentiles.

restrict planning actions to main cable sections. In addition, the decrease of the percentage difference with the PV penetration can be considered as a benefit. Planners may not take actions unless the PV penetration approaches the feeder's hosting capacity limit; only likely to occur at high penetrations [4], where detailed spatial characterization is less required.

Fig. 9 compares the $\Delta P_{flow}[\%]$ values for the random and spatial allocations at a 50% PV penetration. The percentage difference is larger for the spatial allocation. The obtained $\Delta P_{flow}[\%]$, after incorporating PV adoption as a function of the spatial characteristics, can be up to ~6 times greater. Allocations on the network sections can vary highly due to the

Accepted Paper

presence of large PV clusters. In the case of planners performing forecast allocations on a system with similar PV adoption mechanisms, it is important for utilities to have a certain degree of spatial customer characterization. Considering a uniform allocation can result in large under/over estimations of the future system flows over a large portion of the system.

E. Incorporating uncertainty in the total PV forecast

A perfect PV forecast has been assumed up to this point. Consequently, the variations in (5) and (6) originate solely from the allocation models themselves. The propagation of forecast error through the feeder and how it relates to the previous ΔP_{flow} is examined next. For brevity, only the spatial allocation model is considered as it provides the greatest variation from the uniform allocation. For a $PV_{\%}$ of 25 and 50%, 2,500 MC iterations are repeated under different forecast errors. The differences from (5) and (6) are quantified using P_{flow} from all simulations but with $\hat{P}_{flow}$ obtained with no forecast error. Then, ΔP_{flow} is decomposed into a component related to the allocation model and another due to the forecast error:

$$\Delta P_{flow} = \Delta P_{allocation} + \Delta P_{forecast\ error} \quad (6)$$

Results are depicted in Fig. 10 and Fig. 11 for a 25 and 50% PV penetration, respectively, with forecast errors of 10, 20, 30, 40 and 50%. For visualization purposes, as $\Delta P_{forecast\ error}$ is found to follow a normal distribution, only the 90th percentiles are shown (i.e., the positive extreme of the error distribution). In all cases, $\Delta P_{forecast\ error}$ starts with an offset equal to the error at the head of the feeder and varies little across the main cable sections. When approaching the end nodes, $\Delta P_{forecast\ error}$ increases for a low $PV_{\%}$ and decreases for a high $PV_{\%}$. At low penetrations, only a few customers are allocated with PV. Consequently. the extra or less PV allocations due to the forecast error (e.g., an overestimation of the total PV will lead to more PV units to be allocated) increase the range of possible values for P_{flow}; which results on a greater ΔP_{flow}. For both cases, $\Delta P_{forecast\ error}$ converges to zero at the end of the feeder; this is because, for a single customer, any variability is already captured by the allocation model.

Planners can use this analysis to help inform their decision on where to concentrate resources: accuracy of the PV forecast, quality of the spatial information according to the branches of interest, or both. Utilities that focus planning actions at the substation level and upgrade assets near the ending branches because of failure, will find more benefit from improving the quality of their PV forecast rather than their allocation process.

V. Conclusions

Ensuring the feeder models used to plan and design the distribution system are sufficiently representative is an increasing challenge. This paper compares different allocation models and assesses the variability seen in the resulting power flows associated with residential PV adoption. It is shown that such variability depends on the number of aggregated customers, the PV adoption mechanism and the PV penetration level. The study also analyses how the error of the total PV forecast propagates across the allocated powers, differentiating the variability induced by the forecast error from that of the allocation models themselves. This type of analysis can help utilities to decide on whether to concentrate resources on the accuracy of the PV forecast or on the allocation process quality.

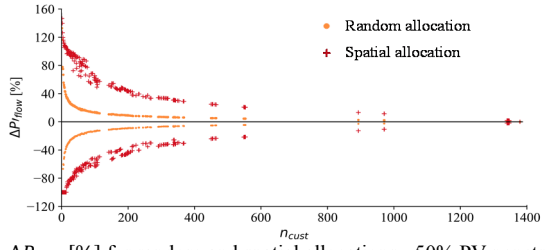

Fig. 9. ΔP_{flow}[%] for random and spatial allocations - 50% PV penetration

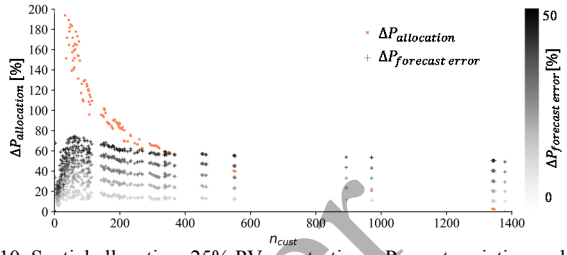

Fig. 10. Spatial allocation: 25% PV penetration – Percent variations related to the allocation method, and to the forecast error (from 10 to 50% in 10% steps)

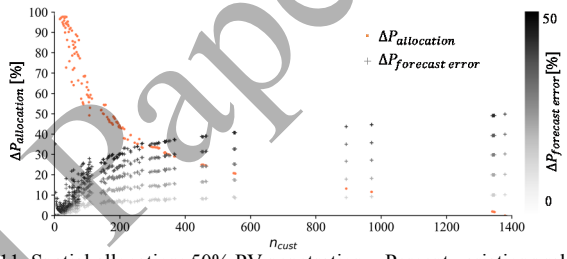

Fig. 11. Spatial allocation: 50% PV penetration – Percent variations related to the allocation method, and to the forecast error (from 10 to 50% in 10% steps)

References

[1] "Distribution Feeder Hosting Capacity : What Matters When Planning for DER ?," *EPRI, Palo Alto, CA 2015. 3002004777.*

[2] A. T. Procopiou and L. F. Ochoa, "Voltage Control in PV-Rich LV Networks without Remote Monitoring," *IEEE Transactions on Power Systems*, vol. 32, no. 2. pp. 1224–1236, 2016.

[3] A. Alarcon-Rodriguez, E. Haesen, G. Ault, J. Driesen, and R. Belmans, "Multi-objective planning framework for stochastic and controllable distributed energy resources," *IET Renew. Power Gener.*, vol. 3, no. 2, pp. 227–238, 2009.

[4] V. Rigoni, L. F. Ochoa, G. Chicco, A. Navarro-Espinosa, and T. Gozel, "Representative residential LV feeders: A case study for the North West of England," *IEEE Trans. Power Syst.*, vol. 31, no. 1, 2016.

[5] H. L. Willis, "Characteristics of distribution loads," in *Electrical Transmission and Distribution Reference Book*, ABB, 1997.

[6] "Enhanced Load Modeling for Distribution Planning: Assessment of Traditional Load Modeling Metrics and Load Allocation Methods using AMI Data," *EPRI, Palo Alto, CA 2017. 3002010995.*

[7] F. Jabari, H. Seyedi, S. Ravadaneg, and B. Mohammadi-Ivatloo, "Stochastic Contingency Analysis Based on Voltage Stability Assessment in Islanded Power System Considering Load Uncertainty Using MCS and k-PEM," in *Handbook of Research on Emerging Technologies for Electrical Power Planning, Analysis, and Optimization: IGI Global*, 2016.

[8] M. Graziano and K. Gillingham, "Spatial patterns of solar photovoltaic system adoption: The influence of neighbors and the built environmentz," *J. Econ. Geogr.*, 2015.

[9] Electric Power Research Institute - EPRI, "Smart Grid Resource Center, EPRI Test Circuits".

[10] Energy Saving Trust, "Solar Energy Calculator Sizing Guide".

[11] S. C. Chapra and R. P. Canale, *Numerical methods for engineers*, vol. 33, no. 3. 2015.

Accepted Paper